

# High Level Battery Modeling Considering Discharge Rate and Temperature Effects

Jingyuan Dong, UCLA, Electrical Engineering.

Advised by Professor Puneet Gupta, UCLA, Electrical Engineering

**Abstract**—A battery is a ubiquitous solution for supplying power in embedded systems. Predicting the residual capacity of a battery is extremely important in the design and application of effective power management policies in portable electronic devices. In this paper, we develop and validate a battery discharge model to predict the battery capacity using Energizer AAAA batteries as a function of discharge rate and temperature for continuous discharging applications. We also analyzed the variability in lifetime of different batteries and found it to be negligible.

**Index Terms**—Battery Modeling, Discharge Rate, Temperature, Individual Variability.

## I. INTRODUCTION

The rapid advancement of modern portable electronics has resulted in the development of devices combining high-speed CPU, high resolution display, fast storage and high-speed wireless data transfer to drive exciting new applications. As a result, these devices consume significantly more energy compared to earlier generations of devices. However, the advances in battery technologies have not kept up with the energy requirements of these electronics.

Since portable devices use batteries as the sole of energy, energy becomes a critical issue in these systems. In addition, the energy consumed in the circuit is not always the same as the energy drawn from the battery [1]. Therefore, studying and understanding battery discharge behavior is important and battery modeling is an essential tool to reach this goal.

When a battery is connected to a load, a reduction-oxidation reaction occurs, resulting in the transfer of electrons from the anode to the cathode. This process converts the chemical potential energy of the battery into electrical energy to drive the electronic circuit. Eventually, the consumption of electroactive species in the battery causes the battery to reach a threshold known as the cutoff voltage. After reaching this voltage, the battery is considered to be depleted.

There are many factors that affect battery capacity. Commonly identified factors include discharge rate, temperature and individual battery variability. In addition, for the rechargeable batteries, the charge-recharge cycles also have a significant impact on the battery capacity.

Developing computationally feasible battery models has been a key research topic for several years. Those models can be largely divided into four different categories: physical models, empirical models, abstract models and mixed models.

They can be evaluated according to their prediction accuracy, computational complexity, configuration effort and analytical insight.

In this paper, we conduct studies on battery discharge behavior. Based on an earlier work [1], we first validate an old battery model. We then modify the battery model to account for the effect of temperature. Finally, we use Energizer AAAA battery discharge data to fit the models and predict the lifetime of the battery. Our results show that the battery model is accurate enough to predict the battery lifetime.

This paper is organized as follows. Section II details prior work on this topic. Section III derives battery models. Section IV details the experimental setup for collecting and verifying data. Section V presents the analysis of the collected battery data. Section VI introduces model fitting and lifetime prediction. Section VII concludes the report.

## II. RELATED WORK

Doyle et. al. [2] developed a physical battery model by studying the isothermal, electrochemical and physical principles within the battery during a single discharge cycle. Solving a set of differential equations, they derived a battery model that described the battery capacity as a function of time. They further validated the model using the Dualfoil platform and FORTRAN simulations. In order to obtain the relevant coefficient for the model, many data configurations are required to determine the precise battery model. Therefore, this model achieves high accuracy but with significant computational complexity.

In [3], a linear-quadratic empirical battery model was developed using the ratio of actual battery capacity and theoretical battery capacity. They averaged the current load and developed an actual battery capacity model corresponding to different loads. The model accurately predicts the effect of different loads on battery capacity. It has relatively small computational complexity and configuration effort. However, the model does not provide high accuracy and only accounts for different discharge rate.

Several researchers have also modeled the battery as electrical circuit. By considering the model as a combination of linear passive elements, voltage sources, and lookup tables that store battery characteristics, they have successfully developed many abstract battery models that have medium accuracy, computational complexity and configuration efforts. In [4], Sean Gold studied the effect of capacity fading on the lifetime

of the battery. They modeled the capacity fading effect as a capacitor, which decreases linearly as the battery cycle increases.

A high-level representation of battery model that combines both experimental data characteristics and physical principles of battery was developed by Rakhmatov et. al. [1]. In the paper, the authors presented a mixed battery model, which is able to predict the battery capacity with high accuracy, medium computational complexity and low configuration efforts. They used Faraday's law for electrochemical reaction and Fick's laws for the 1-D distribution of magnetic concentration to develop the battery model. By solving a series of partial differential equations, they derived a battery model with only two variables. Additionally, they also validated the model by predicting the lifetime of the battery and comparing it with both Dualfoil simulation results and actual measured data.

In this work, we use the mixed battery model [1] to study the battery capacity of Energizer AAAA batteries under continuous discharge, with various discharge current loads. We also study part-to-part variability and temperature-dependent variation in battery capacity using this battery model. Since the mixed battery model accounts for the physical and chemical phenomena within the battery, it has high accuracy and robustness. To validate the battery model, we measure the battery discharge behavior data of Energizer AAAA battery and fit the model with the collected data. We then use the model to predict the lifetime of the battery under different current loads and temperatures. Our measurements indicate very strong temperature dependence of battery capacity but little manufacturing variability in the batteries.

### III. MODEL DESCRIPTION

#### A. Discharge Rate Impact.

Battery capacity depends on discharge rate. As shown in Figure 1(a), before the discharge of any current from the battery, the electrode surface is filled with uniformly distributed electroactive species. When the battery is connected to a load, the electroactive species are consumed and the diffusion process starts. Because the diffusion speed cannot keep up with the consumption speed, a concentration gradient of electroactive species appears across the battery as shown in Figure 1(b). However, when the load is disconnected from the battery, the diffusion process continues and finally reaches equilibrium as shown in Figure 1(c). This is the reason that a battery partially recovers some capacity after a period of rest. At last, as Figure 1(d) shows, after the electroactive species are consumed to a certain level on the electrode, battery reaches the cutoff voltage.

During this process, if the battery discharges rapidly, the consumption speed of electroactive species is much faster than the diffusion speed of the electroactive species. A sharper slope of gradient distribution of the electroactive species appears across the battery. This causes the battery to reach the cutoff voltage rapidly. In comparison, when a battery is being discharged at a slower rate, the difference between the diffusion rate and the consumption rate of the electroactive species is smaller, which results in more electroactive species being

consumed. This is the reason that faster discharge rate leads to shorter battery lifetime while slower discharge rate provides a longer lifetime of battery.

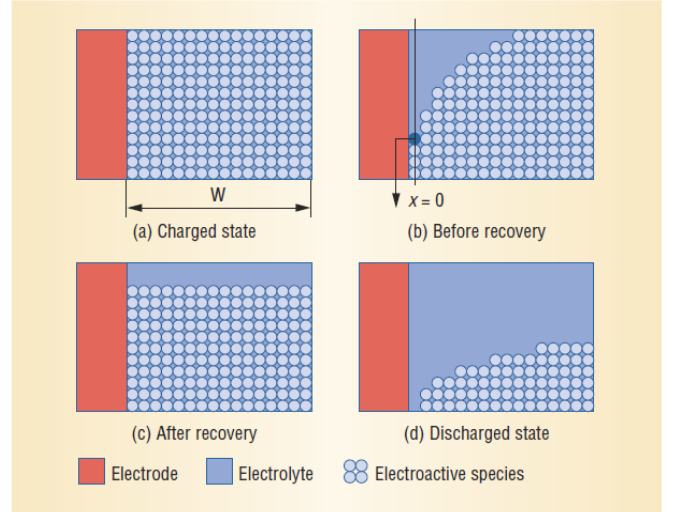


Figure 1: Battery operation in a symmetric, electrochemical cell [5].

#### B. Temperature Impact

Temperature also has a significant impact on the battery capacity. Below room temperature (around 25°C), chemical activity in the battery decreases and internal resistance increases [5]. Thus, at low temperature, the large internal resistance occupies a large part of the output voltage. Compared to a battery with smaller internal resistance, the output voltage reaches the cutoff voltage faster, which decreases the full capacity of the battery. In contrast, high temperature enhances the chemical activity within the battery and decreases the internal resistance. Additionally, the increased chemical activity provides more electroactive species. Therefore, it would take longer to reach the cutoff voltage at high temperature, which increases the battery capacity.

#### C. Individual Variability Impact.

Several aspects of manufacturing may have influences on battery capacity. These factors include the temperature of the manufacturing process, different sources of raw materials and the contamination of the raw materials. These differences between individual batteries would introduce different characteristics. We study part-to-part battery variation by discharging nominally identical batteries with identical loads and operating conditions, and analyzing the resulting lifetime.

#### D. Model Derivation:

Ravishankar et. al. [5] analyzed the battery capacity in a one dimensional diffusion space with a length of  $w$ . Based on Fick's Laws, the authors defined:

$$-J(x,t) = D \frac{\partial C(x,t)}{\partial x} \quad (1)$$

$$\frac{\partial C(x,t)}{\partial t} = D \frac{\partial^2 C(x,t)}{\partial x^2} \quad (2)$$

Applying the boundary conditions, they got:

$$\frac{i(t)}{vFA} = D \frac{\partial C(x,t)}{\partial x} \Big|_{x=0} \quad (3)$$

$$0 = D \frac{\partial C(x,t)}{\partial x} \Big|_{x=w} \quad (4)$$

Solving (1)-(4), the authors obtained an analytical solution and reached a mixed battery model as follows (the details of the derivation can be found in paper [1]):

$$\alpha = \int_0^L i(\tau) d\tau + \lim_{\varepsilon \rightarrow 0^+} 2 \sum_{m=1}^{\infty} \int_0^{L-E} i(\tau) \exp(-\beta^2 m^2 (L-\tau)) d\tau \quad (5)$$

$$\alpha = vFAw(C^* - C_{cutoff}) \quad (6)$$

$$\beta = (\pi \sqrt{D} / w) \quad (7)$$

Under a constant load, this mathematical model can be further reduced to:

$$\alpha = IL \left[ 1 + 2 \sum_{m=1}^{\infty} \frac{1 - \exp(-\beta^2 m^2 L)}{\beta^2 m^2 L} \right] \quad (8)$$

For the more general case where the battery is usually discharging under variable loads, the authors proposed a battery model that is based on equation (8). By considering variable loads as a step wise function of different constant loads, they defined the following model:

$$\alpha = \sum_{k=0}^{N-1} I_k F(L, t_k, t_{k+1}, \beta) \quad (9)$$

where

$$F(L, t_k, t_{k+1}, \beta) = t_{k+1} - t_k + 2 \sum_{m=1}^{\infty} \frac{\exp(\beta^2 m^2 (L - t_{k+1})) - \exp(-\beta^2 m^2 (L - t_k))}{\beta^2 m^2} \quad (10)$$

This is the final model we use in this paper. In order to study the effect of temperature, we analyze the physical meaning of  $\alpha$  and  $\beta$ .

In equation (6), except for the velocity of the electroactive species  $v$ , all other coefficients are constant. So we studied the physical relationship between  $v$  and temperature.

In thermodynamic theory, the kinetic energy usually contributes to all the energy in the molecule. Since molecular energy is  $3/2KT$  and kinetic energy is  $1/2mv^2$ , by equating them, the relationship between  $v$  and temperature is  $v = \sqrt{3KT/m}$ .

In equation (7),  $\pi$  and  $w$  are both constants. The only parameter that has any relationship with temperature is  $D$ . According to Arrhenius dependence on temperature, we get  $\beta^2 = b * \exp(f/T + h)$ . Therefore, we modified the battery model to account for the temperature effect as:

$$\alpha * \sqrt{T} + f = \sum_{k=0}^{n-1} I_k F(L, t_k, t_{k+1}, T) \quad (11)$$

where

$$F(L, t_k, t_{k+1}, T) = t_{k+1} - t_k + 2 \sum_{m=1}^{\infty} \frac{\exp(-be^{(m/T+h)} m^2 (L - t_{k+1})) - \exp(-be^{(m/T+h)} m^2 (L - t_k))}{\beta^2 m^2} \quad (12)$$

TABLE I

PARAMETER DEFINITION

Symbol	Meaning
x	$x \in [0, w]$ is the distance magnetic
J(x,t)	flux of species at time t and at distance x
D	diffusion coefficient
F	Faraday coefficient
L	lifetime of the battery
A	surface area of the electrode
C*	initial concentration of the electroactive species
Cutoff	cutoff concentration of the electroactive species
W	the maximum length of the battery
t	$t \in [0, L)$ is the time

## IV. EXPERIMENTAL SETUP

### A. Data Collection.

In this project, we used Agilent U2722A SMU [6] to record output voltage, internal resistance voltage and current data across time. This device is highly flexible and accurate for such measurements. It has three channels that can collect three different sets of data simultaneously. It can be directly connected to a computer via a USB port and the software package [7] from Agilent can be used to measure battery data at high rates. Figure 2 illustrates the overall architecture of the U2722A SMU and Figure 3 is the Agilent Measurement Manager (AMM) software. For each of the three channels, current source or voltage source can be selected to measure constant discharge current or voltage, respectively. It is also possible to configure the measurement range to collect specific current between  $1\mu A$  to  $120mA$  or voltage between  $0.1V$  to  $2V$ . The AMM also provides a convenient way to record data by enabling the automatic script function that records every measurement into a CSV file.

We initially used SMU and AMM to collect data. However, the measurement process was not controllable and the measured data was not accurate enough. We then developed scripts to control and interact with the SMU for the measurement.

The Agilent U2722A SMU supports SCPI and IVI-COM standard that is compatible with a wide range of ADE. SCPI, also known as the Standard Commands for Programmable Instruments, is an ASCII-based instrument command language designed for test and measurement instruments [8]. It is widely supported in measurement instruments. In particular, there is an Instrument Control Toolbox in Matlab that supports various communication protocols between measurement instruments and computer including GPIB, Serial, TCP/IP, UDP and VISA. GPIB is the most widely used protocol in measurement instruments. Many Agilent instruments support GPIB. However, the U2722A SMU only supports VISA protocol. Thus, in our measurements, we have used this protocol to control the SMU.



Figure 2: Agilent U2722A SMU [6].

Through this VISA protocol and SCPI commands, we develop a script that starts by setting up a new VISA connection by specifying the instrument vendor and the USB port number. The script then clears the previous commands in the device and resets the device. After these configurations, any control commands can be sent to the device and all received data can be stored on the computer. Additionally, by using the Matlab syntax, we can have more control over the SMU. For example, we can enable the device executing a command for a certain amount of time. Finally, the script closes and deletes the connection. The following is a pseudo-code example for measuring battery discharge behavior:

```
obj=visa('AGILENT',
'USB0::0x0957::0x4118::MY51220005::0::INSTR');
fopen(obj); % Open the interface
fprintf(obj, '*CLS'); % Clear the command in the device
fprintf(obj, '*RST'); % Reset the device

%send command to measurement instruments
%receive data from measurement instruments

fclose(obj); %close the connection
delete(obj); %delete the connection
clear obj;
```

Using this script, we designed different measurement plans. According to the specification of the SMU, we measured the output voltage under four different constant current loads: 60mA, 80mA, 100mA and 120mA. We first measured different constant current loads at the room temperature. The result showed that 60mA and 80mA loads took 9 and 7 hours to exhaust the battery, respectively. In order to accelerate the data measurement process we collected data under 100mA and 120mA constant loads for various temperatures. Considering the operation temperature of the battery, we measured 100mA and 120mA constant loads at 0 Celsius, 20 Celsius, 40 Celsius and 55 Celsius.

Before starting the measurements, we must study the individual variability for Energizer AAAA battery. In this way, we can ensure that the real average battery capacity would have a reasonable probability lying in the range that is obtained from the measurement data. We then can determine the number of data samples needed to meet the requirements.

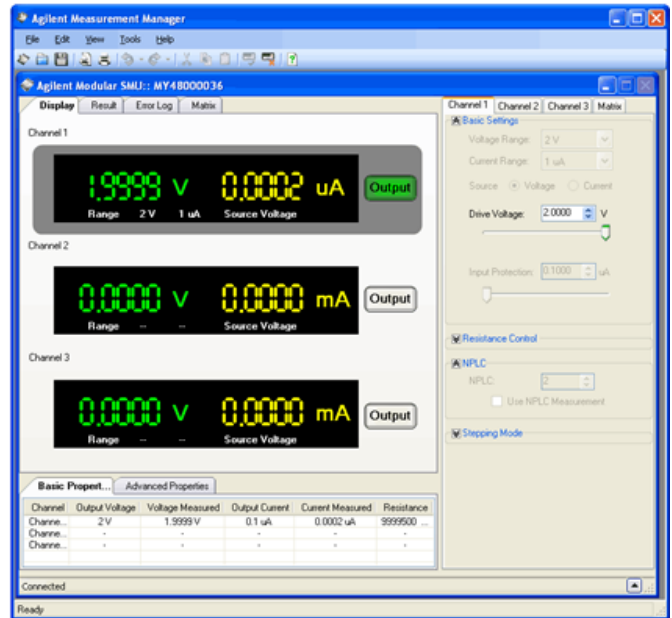


Figure 3: Agilent Measurement Manager [7].

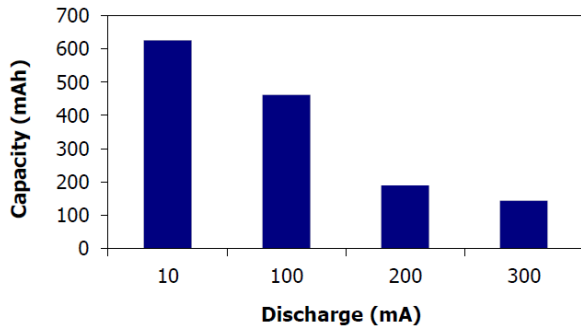
### B. Data Verification.

After the data was collected, we verified it to ensure its correctness. Figure 4(a) shows the battery capacity according to the Energizer AAAA datasheet [9]. Under 100mA discharge rate at room temperature, it has a battery capacity of about 450mAh, which means that the battery has a lifetime of about 4.5 hours when it is discharging at a rate of 100mA. In Figure 4 (b), the X-axis is the lifetime of the battery in seconds and the Y-axis is the output voltage of the battery. It shows a general battery discharge behavior under 100mA. Since the datasheet of the Energizer AAAA battery defines the cutoff voltage to be 0.8 volts, we terminated the measurement process when the output voltage reached 0.8V. The result shows it took 16729 seconds which is approximately 4.65 hours to reach this cutoff voltage. This value is close to the data sheet value with only 3.33% error.

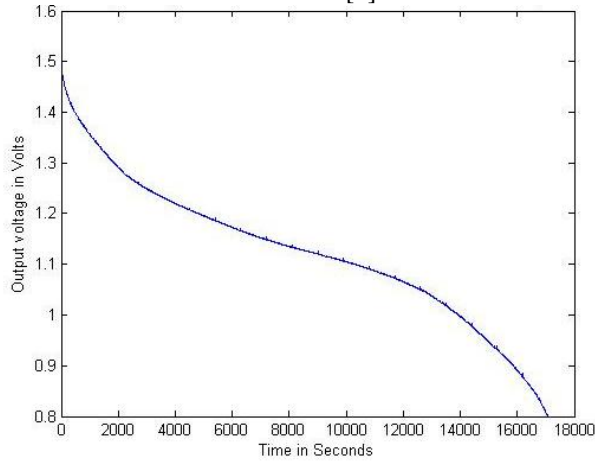
Figure 5(a) shows the battery performance under constant discharge rate from [9]. It shows that the service hour of the battery is between 9 hours and 4.8 hours in the current range between 60mA and 100mA. In Figure 5(b), the X-axis is the discharge current load over four different values and Y-axis is the lifetime for each individual current load. We converted the lifetime of the battery into hours and calculated a linear regression for the battery lifetime and current load as  $Y = -0.08829 * X + 13.93$ . Considering the service hour for the battery being discharged between 60mA and 100mA, we can conclude that the overall performance matches with the manufacturer's specification well under different current loads at room temperature. Therefore, using the script to collect battery output voltage will produce sufficiently accurate data. Later on, we used the same script to measure all the battery discharge data for different situations.

### Milliamp-Hours Capacity

Continuous discharge to 0.8 volts at 21°C



(a): Battery capacity and discharge rate relationship from datasheet [9].



(b) Battery discharge behavior for 100mA

Figure 4. Comparison between measured data and datasheet specification for lifetime under 100mA.

### V. DATA ANALYSIS AND MODEL VALIDATION

After data verification, the analysis of the data was performed using three steps. The first step is to study the individual variability of the battery. The second step is to study the effect of different current loads on the battery model. The third step is to study the effect of temperature on the battery model.

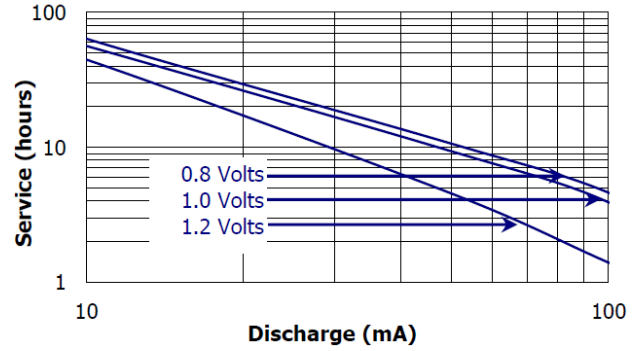
#### A. Variability Study

Due to various factors, batteries exhibit individual variability in energy capacity. For example, variability in the battery manufacturing processes can lead to differences in the mixture ratio of raw materials. Variability can also be caused by differences in battery manufacturing temperature and in different factories having variation in processing equipment. Thus, in order to obtain the correct data that demonstrates the real battery discharge behavior, we must study the individual variability. We use probability theory to study the expected lifetimes and expected energy capacities. We also calculate the confidence interval for lifetime and energy. From our analysis, we found that the individual variability in Energizer AAAA batteries is negligible and does not significantly influence the battery capacity.

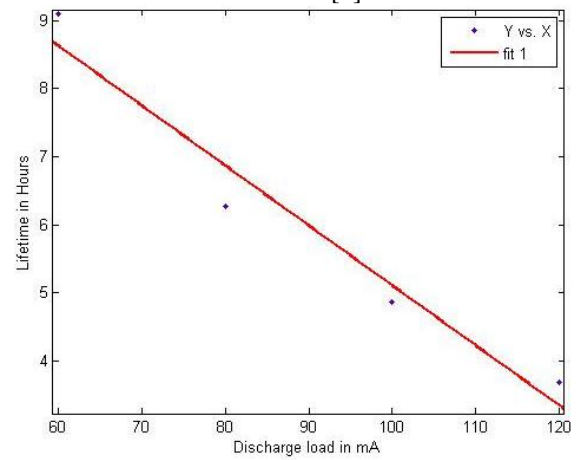
In Figure 6, the X-axis is the lifetime of the battery in

### Constant Current Performance

Typical Characteristics (21°C)



(a) Battery lifetime and discharge rate relationship from datasheet [9].



(b) Measured and fitted battery performance under constant current.

Figure 5. Comparison between measured data and datasheet specification for lifetime under different discharge rates.

seconds and the Y-axis is the open circuit voltage in volts. There are 12 data samples to show the discharge behavior of 12 batteries. It is clear that all 12 samples demonstrate almost identical discharge behavior with very little difference in energy and lifetime.

In addition, we studied the individual variability of these batteries at 60mA, 80mA and 100mA. The results show the same characteristics. Thus, we do not plot that data in this report. Furthermore, we analyzed the data in terms of expected value and standard deviation for lifetime and energy capacity. The results are shown in Table II.

As Table II shows, compared with the expected lifetime, the standard deviation of the lifetime is around 1%. The same relationship can be found between the expected energy capacity and standard deviation of energy capacity. This means that there is no significant variability in either lifetime or energy capacity. In addition, in order to have a deeper understanding of the data, we calculated the confidence interval (CI) for battery lifetime and energy capacity. We used the definition of mean value confidence interval that  $\Pr(\mu - c\sigma'/\sqrt{n} < x < \mu + c\sigma'/\sqrt{n}) = r$  where  $\mu$  is the expected value of the samples,  $c$  is the look up value in t distribution,  $\sigma'$  is the unbiased estimation of standard deviation,  $N$  is the degrees of freedom,  $r$  is the confidence probability. We also used the definition  $[(n-1) \times S^2 /$

$\chi^2\alpha/2, n-1] \leq \sigma^2 \leq [(n-1) \times S^2 / \chi^2 1-\alpha/2, n-1]$  to calculate the standard deviation confidence interval. We calculated the confidence interval for expected value with 95% confidence level and confidence interval for standard deviation with 90% confidence level. All results are shown in Table III. As this table also shows, the variability of the battery is small. Thus, correct battery discharge behavior can be obtained via limited number of data samples. Hence, we conclude that the battery variability does not have a significant impact on the battery discharge behavior.

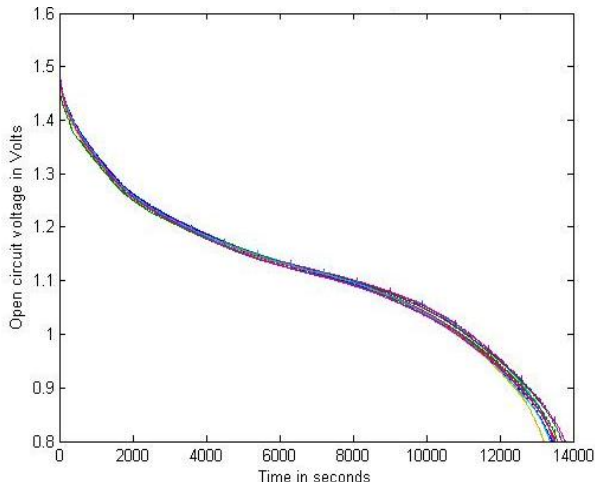


Figure 6: Battery discharge behavior under 120mA at room temperature for 12 battery samples

### B. Discharge Rate Study:

We now analyze the effect of discharge rate on the battery model. Figure 7 shows the battery discharge behavior under different discharge rates at room temperature. From the figure, it is clear that a faster discharge rate results in a much shorter lifetime while a slower discharge rate provides a longer lifetime. In addition, we also calculated the energy capacity of the battery over different discharge rates. The results are shown in Figure 8. From the figure, it is clear that the battery capacity, in terms of energy capacity, does not change linearly with the discharge rate. Large discharge rate results in small energy capacity. However, if the discharge rate is small, the energy capacity increases exponentially.

### C. Temperature Study

As we discussed earlier, temperature has a significant influence on the battery capacity. Thus, we analyze the effect of temperature on the battery model. Figure 9 and Figure 10 illustrates this temperature effect on the battery discharge behavior under 100mA and 120mA, respectively. The two figures show the same behavior with respect to temperature for both 100mA and 120mA. When the temperature is below room temperature, the battery capacity decreased dramatically. In the case of 0 Celsius, the discharge slope is sharp and the battery dies quickly. However, above room temperature, the battery capacity increases slowly. This trend is shown in Figure 11. As we can see from the figure, 100mA and 120mA discharge rates show the same relationship between the battery capacity and temperature. Furthermore, the relationship of both energy and lifetime with temperature has similar characteristics. The

capacity increases rapidly at first and then saturates when the temperature becomes high.

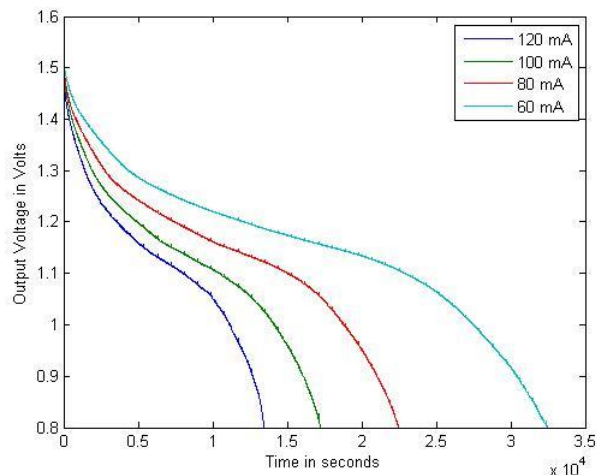


Figure 7: Battery discharge behavior under different current load at room temperature.

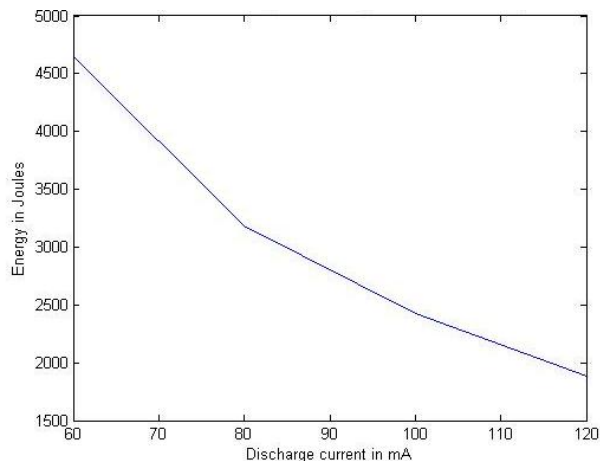


Figure 8: Energy and discharge current relationship at room temperature.

## VI. MODEL FITTING AND LIFETIME PREDICTION

In the first step, we validate the battery model in Equation (9) and (10) for different discharge rates. Since lifetime is not a fixed number but can be obtained through the measured data, we have to change the model to the following form:

$$I_k = \frac{\alpha}{L_k + 2 \sum_{m=1}^{10} \frac{1 - \exp(-\beta^2 m^2 L_k)}{\beta^2 m^2}} \quad (13)$$

Since we already know the discharge profile, we can use the least square approximation to get the optimal value of  $\alpha$  and  $\beta$  with the following equation:

$$\sum_{k=1}^M (I_k - I_{realK})^2 \quad (14)$$

where  $I_k$  is the current we calculated through the model and  $I_{realK}$  is the measured current data. By minimizing this least squares error using gradient descent, we can get the optimal value for  $\alpha$  and  $\beta$ .

Table II. Comparison between expected lifetime/energy and standard deviation of lifetime/energy.

	$\mu$ value for lifetime(Sec)	$\delta$ for lifetime	Error rate ( $\delta/\mu$ )	$\mu$ value for energy capacity (Joule)	$\delta$ for energy capacity	Error rate ( $\delta/\mu$ )
120mA	1.3445e+004	177.3	1.32%	1.8880e+003	21.0	1.11%
100mA	1.7334e+004	444.2	2.56%	2.4218e+003	49.1	2.03%
80mA	2.2576e+004	307.1	1.36%	3.1839e+003	42.8	1.34%
60mA	3.2777e+004	231.2	0.71%	4.6499e+003	34.0	0.73%

Table III. Mean confidence interval and standard deviation confidence interval for battery lifetime and battery energy.

	$\mu$ CI (Lifetime)	$\delta$ CI (Lifetime)	$\mu$ CI (Energy capacity)	$\delta$ CI (Energy capacity)
120mA	13344.68 - 13545.32	132.570 - 274.928	1876.1 - 1899.9	15.7 - 32.5
100mA	17043.79 - 17624.21	319.047 - 760.033	2389.9 - 2454.1	35.3 - 84.1
80mA	22228.49 - 22923.51	206.386 - 641.611	3135.6 - 3232.4	24.7 - 188.9
60mA	32515.38 - 33038.62	155.378 - 483.036	4611.5 - 4688.5	19.7 - 150.1

Table IV. Model fitting results for different discharge rates.

	60mA	80mA	100mA	120mA	60mA and 120mA (Periodically exchange value every 15 minutes)
Measurement lifetime in Minute	546.28	376.27	285.55	221.32	290.00
Model predicted lifetime in Minute	465	345	270	225	300
Error	14.84%	8.31%	5.45%	1.66%	3.45%

Table V. Model fitting results for different discharge rates accounting for the impact of temperature.

	60mA (20C)	80mA (20C)	100mA (0C)	100mA (20C)	100mA (40C)	100mA (55C)	120mA (0C)	120mA (20C)	120mA (40C)	120mA (55C)	60mA - 120mA 15 min periodically change (25C)
Measured lifetime in minutes	546.28	376.27	117.28	285.55	326.13	329.27	85.04	221.32	256.37	260.02	290
Predicted lifetime in minutes	455.1	341	108	271	317	354	81.1	225	263	294	270
Error	16.69%	9.37%	7.91%	5.09%	2.80%	7.50%	4.64%	1.67%	2.59%	13.08%	6.89%

A Matlab program is written to implement this. First two arbitrary initial values were chosen for  $\alpha$  and  $\beta$  along with an initial step size  $c$ . At each step of the gradient descent iteration, we update the value of  $\alpha$  and  $\beta$  by computing the gradient. To ensure that the step size is not too large, we first define gradient difference height as the sum of the two gradients for each variable. If the difference between the new values and the old values of  $\alpha$  and  $\beta$  is smaller than half the gradient difference height, we accept the new values. Otherwise we decrease the value of  $c$  until the new values meet the criteria. Finally, when the product of the gradient and coefficient  $c$  is smaller than a threshold value, we terminate the iterations. The values of  $\alpha$  and  $\beta$  obtained after this least squares fitting are used in our battery model.

After the value of  $\alpha$  and  $\beta$  are obtained, we use the model to predict the lifetime of the battery. First, we define a function  $f(x)$  as follows:

$$f(x) = \alpha - \sum_{k=0}^{u-1} I_k F(x, t_k, t_{k+1}, \beta) - I_u F(x, t_u, x, \beta) \quad (15)$$

where  $u$  is the current discharge step and  $f(x)$  stands for the remaining capacity of the battery.

We define the first time  $f(x)$  reaches 0 as the lifetime of the battery. Thus, given the discharge profile, we can now systematically calculate the lifetime of the battery. The results are shown in Table IV.

As Table IV shows, the error between the predicted lifetime and measured lifetime is within a reasonable range. Specifically, the heavy discharge rate has an error under 5% while the light discharge rate has an error under 15%. This result matches the results of Rakhmatov et. al. [1]. Furthermore, we studied the case where the battery is discharging under varying discharge rate. We chose a load profile that periodically oscillates between 60mA and 120mA

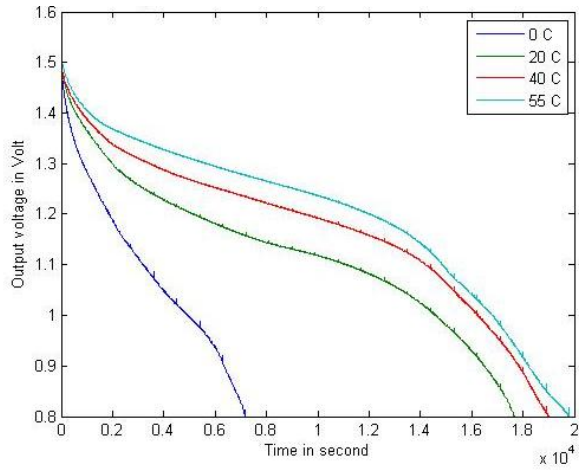


Figure 9. Battery discharge behavior in various temperatures under 100mA.

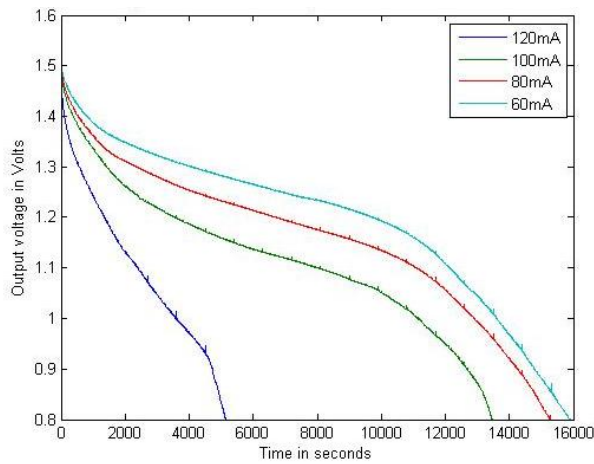


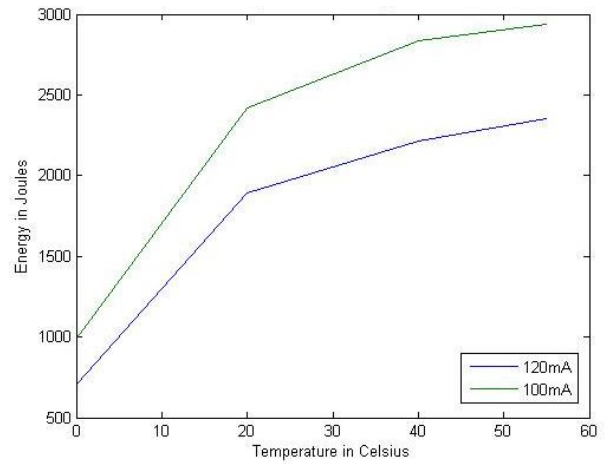
Figure 10. Battery discharge behavior in various temperatures under 120mA.

with a time period of 15 minutes. As Table IV shows, the error rate is within 5%, which means that the model works even for time varying discharge rate. Figure 12 illustrates this scenario.

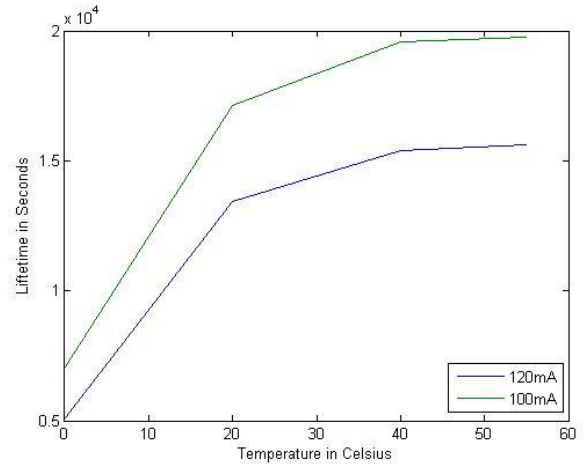
In the second step, we fitted the temperature model defined by Equation (11) and (12). The gradient descent optimization described earlier is used again with slight modifications to account for the specific data in this scenario. The fitted data is shown in Table V, along with the prediction error. As shown Table V, and illustrated in Figure 13, even after modifying the battery model to account for temperature, lifetime prediction error does not change significantly.

## VII. CONCLUSION

In this work, we experimentally measured the lifetime of several batteries under different discharge conditions. Using this measured data we analyzed the variability in battery capacity across 12 samples. We also analyzed the impact of discharge rate and temperature on the battery capacity. In addition to this, the battery model to predict battery lifetime proposed by Rakhmatov et. al. [1] was fitted and validated for different discharge rates. We proposed a modification to this model that accounts for the impact of temperature on battery life. The predicted lifetime of this model matches well with



(a) Energy temperature relationship



(b) Lifetime temperature relationship

Figure 11. Energy/Lifetime and temperature relationship under 100mA and 120mA

the experimental data. This improved model can therefore be incorporated as a part of power management in portable embedded systems.

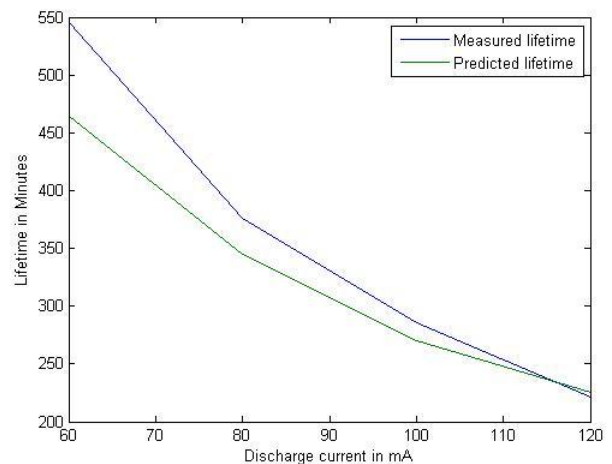


Figure 12. Comparison between measured and predicted lifetime under different discharge current at room temperature.



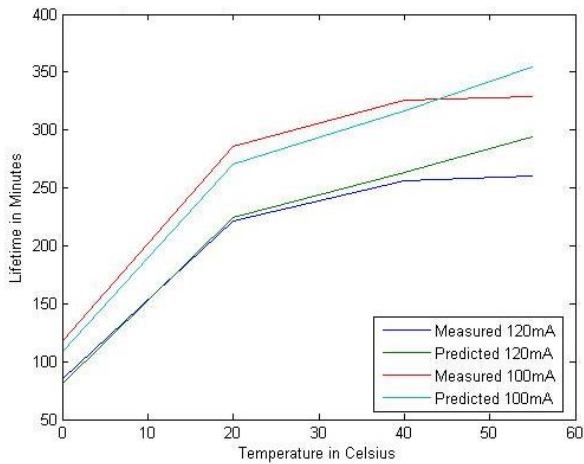


Figure 13. Comparison between predicted and measured lifetime under 100 mA and 120mA under different temperatures

#### ACKNOWLEDGEMENT

I would like to show my gratitude to Professor Puneet Gupta for his kindness, guidance, support and help throughout the project. I would also like to thank Shaodi Wang, Liangzhen Lai and Lucas Wanner for their support and help.

#### REFERENCE

- [1] D. Rakhmatov, S. Vrudhula, and D.A. Wallach, "A Model for Battery Lifetime Analysis for Organizing Applications on a Pocket Computer," IEEE Trans. on VLSI Systems, vol. 11, no. 6, 2003.
- [2] M. Doyle, T.F. Fuller, and J. Newman, "Modeling of Galvanostatic Charge and Discharge of the Lithium/Polymer/Insertion Cell," J. Electrochemical Soc., vol.140, no. 6, 1993, pp. 1526-1533.
- [3] M. Pedram and Q. Wu, "Design Considerations for Battery-Powered Electronics," Proc. 36th ACM/IEEE Design Automation Conf., ACM Press, 1999, pp. 861-866.
- [4] S. Gold, "A PSPICE Macromodel for Lithium-Ion Batteries," Proc. 12th Ann. Battery Conf. Applications and Advances, IEEE Press, 1997, pp. 215-222.
- [5] Ravishankar Rao, Sarma Vrudhula and Daler N. Rakhmatov, "Battery Modeling for Energy Aware System Design" IEEE trans. on Computer, Vol.36 Issue, 12, 2003, pp. 77-87.
- [6] [http://www.home.agilent.com/upload/cmc\\_upload/ck/zz-migration/images/U2722A\\_EC.jpg](http://www.home.agilent.com/upload/cmc_upload/ck/zz-migration/images/U2722A_EC.jpg)
- [7] [http://www.home.agilent.com/upload/cmc\\_upload/All/U2722A.gif](http://www.home.agilent.com/upload/cmc_upload/All/U2722A.gif)
- [8] U2722A\_U2723A programmer's reference.
- [9] <http://data.energizer.com/PDFs/E96.pdf>, Energizer AAAA battery data sheet.